In-situ nanodiamond to carbon onion transformation in metal matrix composites

Sebastian Suarez, Leander Reinert, Marco Zeiger, Patrice Miska, Samuel Grandthyll, Frank Müller, Volker Presser, Frank Mücklich

Formal publication in *Carbon*, https://doi.org/10.1016/j.carbon.2017.12.072

In-situ nanodiamond to carbon onion transformation in metal matrix composites

Sebastian Suarez[1,], Leander Reinert[1,2], Marco Zeiger[3,4], Patrice Miska[5], Samuel Grandthyll[6], Frank Müller[6], Volker Presser[3,4], and Frank Mücklich[1,2,*]*

[1] Functional Materials. Department of Materials Science and Engineering, Saarland University, Campus D3 3, 66123, Saarbrücken, Germany.

[2] Materials Engineering Center Saarland (MECS), Campus D3 3, 66123, Saarbrücken, Germany.

[3] Energy Materials, Department of Materials Science and Engineering, Saarland University, Campus D2 2, 66123 Saarbrücken, Germany.

[4] INM - Leibniz Institute for New Materials, Campus D2 2, 66123 Saarbrücken, Germany.

[5] Institute Jean Lamour, CNRS UMR 7198, Université de Lorraine, Nancy, F-54000, France.

[6] Experimental Physics, Saarland University, Campus E2 9, 66123 Saarbrücken, Germany.

Abstract

In the present study, nickel matrix composites reinforced with a fine distribution of nanodiamonds (6.5 vol%) as reinforcement phase are annealed in vacuum at different temperatures ranging from 750 °C to 1300 °C. This is carried out to evaluate the in-situ transformation of nanodiamonds to carbon onions within a previously densified composite. The resulting materials are thoroughly analyzed by complementary analytical methods, including Raman spectroscopy, transmission electron microscopy, scanning electron microscopy, energy dispersive X-ray spectroscopy and X-ray photoelectron spectroscopy. The proposed in-situ transformation method presents two main benefits. On one hand, since the particle distribution of a nanodiamond-reinforced composite is significantly more homogenous than in case of the carbon onions, it is expected that the transformed particles will preserve the initial distribution features of nanodiamonds. On the other hand, the proposed process allows for the tuning of the sp^3/sp^2 carbon ratio by applying a single straightforward post-processing step.

**Corresponding authors. Tel: +49 681 30270538. E-mail: s.suarez@mx.uni-saarland.de (Sebastian Suarez)*
Tel: +49 681 30270500 E-mail: muecke@matsci.uni-sb.de (Frank Mücklich)

1. Introduction

Carbon nanoparticles, in their wide variety, are found in numerous technological applications covering fields ranging from nanoelectronics to medicine, among several others. Specifically, sp^2-hybridized nanocarbons have been thoroughly investigated in the last three decades [1]. Two particularly interesting nanocarbons are nanodiamonds as well as carbon onions. Nanodiamonds are sp^3-hybridized carbon nanoparticles with a lattice spacing of about 0.21 nm and a primary particle diameter of around 5 nm (i.e., quasi zero dimensional) [2]. They have been synthesized by a variety of different methods like detonation technique, laser ablation, ultrasound cavitation and others [2]. Intrinsic properties such as superior hardness and Young's modulus, high thermal conductivity, electrical resistivity, and chemical stability demonstrate the high potential of this carbon nanomaterial [2,3]. Beside applications for example in the medical sector, nanodiamonds are promising to reinforce metallic composites. In this regard, nanodiamonds have shown high performances by increasing hardness as well as wear resistance [4–6].

Carbon onions (also called onion-like carbon, OLC) are multi-layered fullerene-like polyhedral nanoparticles [7]. By varying the synthesis method and its parameters, both, the sp^3 to sp^2 carbon ratio and the atomic arrangement can be adjusted. Carbon onions provide a high electrical conductivity [3], large surface area because of their nanometer-size (typically 5-10 nm), and very good mechanical properties [7]. Thus, the particles are used as reinforcement phase for composite materials [8], for tribological lubrication [9], electrochemical energy storage [10], or water treatment [7].

Nanodiamonds obtained from a detonation process are often used as starting materials in the thermal synthesis of carbon onions. Thermal annealing in a temperature range above 700 °C under vacuum or inert gas atmosphere allows to tune the sp^2/sp^3 ratio and modify, accordingly, properties like the electrical conductivity [7,11,12]. Regarding the mechanical and tribological properties, sp^3-hybridized carbons are rather known for its hardness and its resistance to wear [6,13], whereas sp^2-hybridized carbons are usually associated with lubricity and friction reduction [14,15]. For an extended overview of the physical properties of both nanoparticles, please refer to the work of Mochalin et al. [2] and Zeiger et al. [7] and references therein.

A way of capitalizing on the properties of these nanodiamonds and carbon onions with macroscopic materials is by using these carbon nanoparticles as reinforcement phase in metal matrix composites (MMC). One of the major challenges during the manufacturing of this type of MMC is the carbon nanoparticle agglomeration. Particularly, if the selected fabrication route is the solid state processing (i.e., sintering), the mass transport leads to densification and results

in an increased agglomerate formation [16]. This may lead to a poor interface between matrix and reinforcement, decreasing the potential enhancement of the physical properties. To obtain an optimum reinforcing effect, microstructural tailoring can be applied to avoid or minimize nanoparticle agglomeration. This can be achieved by modifying the microstructure in several ways. First, during densification in solid-state routes, the homogeneous distribution of a reinforcement phase pins the grain boundaries, resulting in a smaller mean grain size and increased strength. Second, during application, the particle dispersion acts on the dislocation mobility, reducing it and increasing the thermal stability of the microstructure [17]. Third, in tribological applications, the homogeneous and continuous release of carbon nanoparticles from the MMC towards the contact region can be beneficial and may be optimized in materials with a homogeneous distribution of the reinforcement phase.

In previous studies, it has been shown that sp^2-hybridized carbon nanoparticles form agglomerates faster and to a higher degree than their sp^3-hybridized counterparts mainly due to van der Waals interactions [8]. Additionally, nanodiamonds have shown good colloidal stability in ethylene glycol, which serves as a precursor for MMC fabrication [8]. This further translates to an improved distribution homogeneity of nanodiamonds in the metal matrix, compared to carbon onion reinforced MMC processed by the same route [18]. Considering the different material properties of these two carbon nanoparticles, it is of high interest to produce carbon onion reinforced MMC with the same distribution homogeneity as nanodiamonds to enable wider application flexibility. One possibility to increase the dispersion and distribution of carbon nanoparticle is the chemical modification of surface functional groups (covalent or non-covalent) [19]. However, a covalent functionalization (e.g., with hydroxyl, carboxyl or carbonyl groups) implies the breaking of covalent carbon bonds; thus, compromising the structural integrity of the particles and affecting their intrinsic properties [20,21]. A non-covalent functionalization involves the use of surfactants, polymers, or molecule wrapping [22–25]. The main drawback of this route is that, after processing at high temperatures (e.g., sintering), these additional products remain degraded by-products at the reinforcement-matrix interface, significantly hindering the load/charge transfer capability of the composite.

The present study explores a straightforward technique to overcome the limitations in the dispersion and distribution homogeneity of carbon onions as reinforcement material in MMC, avoiding the use of any chemical functionalization. This is done by thermal treatment of already densified nanodiamond reinforced MMC to trigger in-situ the nanodiamond to carbon onion phase transformation. Furthermore, as the annealing temperature allows to tune the sp^2/sp^3-ratio, the material properties of the composite can be adapted to match the requirements for

different applications. The analysis is supported by a wide span of advanced characterization methods, including Raman spectroscopy with ultraviolet laser radiation, transmission electron microscopy (TEM), scanning electron microscopy (SEM), energy dispersive X-ray spectroscopy (EDS), and X-ray photoelectron spectroscopy (XPS).

2. Materials and methods

Nanodiamond powder was purchased from NaBond Technologies Co., with a carbon purity 98-99% and individual particle diameter 4-6 nm. For the composite manufacturing, the nanodiamonds were dispersed in ethylene glycol (0.1 mg/mL) by shear mixing (5 min) and ultrasonication (20 min). For this process, a homogenizer UltraTurrax (IKA-Werke GmbH) and an ultrasonic bath from Bandelin (Sonorex Super RK 514 BH, 860 W, and 35 kHz) were used. After dispersion, Ni dendritic powder (AlfarAesar, -325 mesh) was added and mixed again by shear mixing for 5 min to achieve a mixture of 6.5 vol% of nanodiamonds in nickel powder. Subsequently, the solvent was evaporated at 150 °C and the obtained powder is pre-densified to green cylindrical pellets with a diameter of 8 mm using a uniaxial press (990 MPa pressure). This step was followed by hot uniaxial pressing in vacuum ($2 \cdot 10^{-4}$ Pa) at a temperature of 750 °C, using a pressure of 264 MPa for 2.5 h and a heating and cooling rate of 20 °C/min. Using these parameters, a final relative density of 98 % was achieved. Only few materials qualify for the choice of the matrix material since metals that readily react with carbon (e.g., Al, Ti, Cr) might affect the evaluation. In this case, Ni was selected as the matrix material, since it does not form stable carbides (a consequence of the carbon nanoparticle degradation) under the studied range of conditions. The only carbide formed by Ni is of metastable nature in a wide temperature range. Ni_3C is, among all possible carbides, the one with the lowest formation energy (26.36 kJ/mol) [26].

The already densified nanodiamond-reinforced samples are then post-processed by an annealing step under vacuum (10^{-3} Pa) at 750 °C, 900 °C, 1100 °C, and 1300 °C, each for 3 h of holding time with a heating and cooling rate of 10 °C/min. It is not possible to investigate higher transformation temperatures (1700 °C, as reported in [27], where high graphitization is achieved) due to the limitation given by the melting temperature of the matrix material ($T_{m,\,Ni}$ = 1453 °C).

Characterization of the samples was done by TEM using a JEOL 2100F transmission electron microscope operated at 200 kV. Small fractions of the samples were removed by scratching and dispersed in isopropanol. These fractions are deposited onto Cu grids coated with lacey carbon for their subsequent TEM analysis.

Raman spectroscopy was performed using a Horiba UV-Raman spectrometer, working with an excitation laser wavelength of 325 nm (3.81 eV). The choice was made since UV excitation is more sensitive to sp^3-hybridized carbons than visible light [28]. The laser power on the sample was 5 mW and the in-focus-plane spot size of approximately 5 µm. The used numerical aperture was 0.5 and we chose a grating of 2400 lines/mm, resulting in a spectral resolution of 1.2 cm^{-1}. For the analysis, the spectra were fitted with Lorentz functions. The reported peak parameters correspond to those of the fitted functions.

SEM and EDS analyses were performed using a dual beam focused ion beam/field emission scanning electron microscope workstation (FEI Helios NanoLab 600). SEM micrographs were recorded with an accelerating voltage of 5 kV and current of 1.4 nA.

The XPS measurements were performed with an ESCA MkII spectrometer (Vacuum Generators) in normal emission mode using Al-K_α excitation ($\hbar\omega$ = 1486.6 eV) and a 150°-type hemispherical analyzer with a pass energy of 20 eV. The calibration was made to the Au-4f 7/2 line at 83.80 eV. The acquired C-1s spectra of the samples treated at 750 °C and 1300 °C were fitted with four Gaussian distributions corresponding to sp^2, sp^3, C-O, and C=O bonded carbon. Both spectra were fitted simultaneously, meaning that for each carbon species, the binding energy as well as the width of the corresponding peak are the same in both spectra, that is, both spectra just differ in the distribution of peak heights.

3. Results and discussion

The UV-Raman characterization provides detailed insights into the transformation steps from nanodiamond to carbon onions within the composite [29]. **Figure 1** shows the evolution of the transformation of nanodiamond at different processing temperatures.

The initial state presents three peaks at 1097.8 cm^{-1}, 1325.8 cm^{-1}, and 1637.2 cm^{-1}, which correspond to pure nanodiamond powder. The first peak at low wavenumbers is assigned to the presence of partially crystalline diamond [30], whereas the second peak is typically identified as crystalline diamond. The third peak (higher wavenumber) is an upshifted G band, moved by the convolution of the peaks generated by C=C, O-H, and C=O bonds [31].

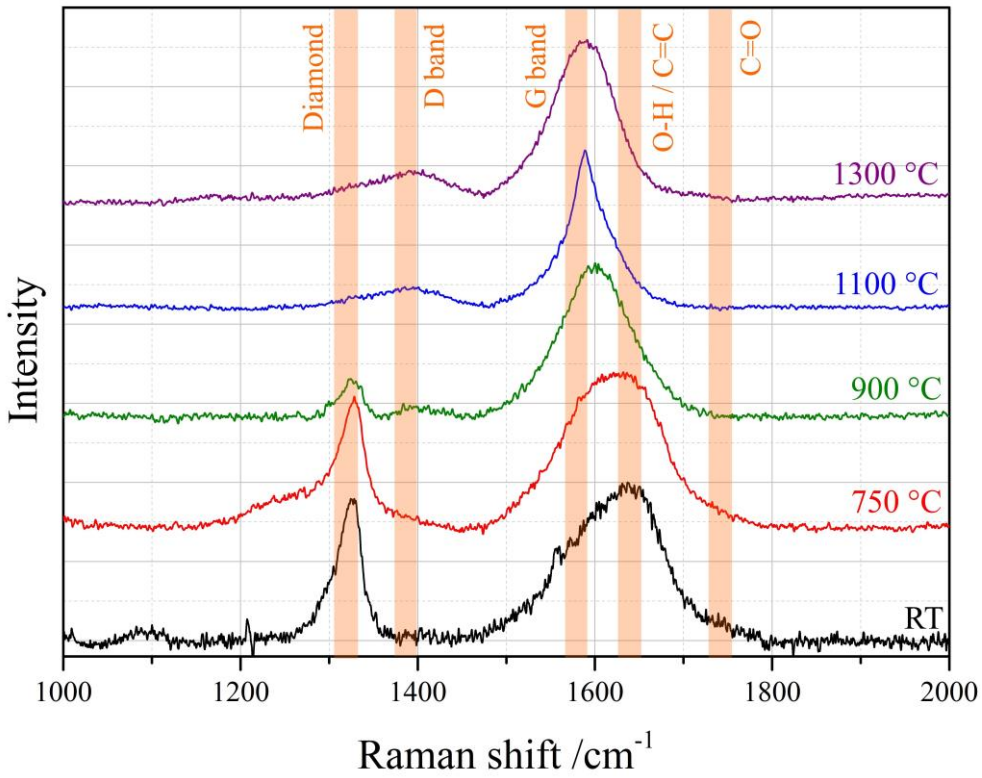

Figure 1 – Raman spectra of nanodiamond reinforced Ni composites at different post synthesis treatment temperatures. The characteristic bands are highlighted in orange.

The reported temperatures for the sp^3/sp^2 transformation range from 670 °C to 1000 °C and depend strongly on the synthesis method and surface chemistry of the nanodiamonds [7,32,33]. The first selected temperature (750 °C) is usually applied to densify this type of composites by hot uniaxial pressing in vacuum [34] and is above the onset temperature for graphitization observed by differential scanning calorimetry by Xu et al. [35]. At this temperature, the low wavenumber peak observed at room temperature vanishes, and a new peak appears at 1236.8 cm^{-1} that can be related to the signal combination of large and small domain scattering [2]. Yushin et al. assign this peak to partially crystalline diamond, which does concur with a short-range order scattering type [30]. The other two observed peaks correspond to the diamond band (1328.3 cm^{-1}) and the upshifted G-band of sp^2-hybridized carbon (1624.1 cm^{-1}).

By increasing the temperature to 900 °C, the transformation from sp^3- to sp^2-hybridization becomes more evident in alignment with the work of Cebik et al. [36]. Three peaks are observed at 1326.4 cm^{-1}, 1395.4 cm^{-1}, and 1600.7 cm^{-1}, with the first band assigned to diamond, the second to the D-band and the last to the upshifted G-band of sp^2-hybridized carbon. Moreover, the intensity of the diamond band is clearly reduced. In this case, the position of the G-band is in agreement to what was reported by Ferrari and Robertson [28]; the latter work assigned the position of the G-band at 1600 cm^{-1} to a nanocrystalline-graphite. This upshift is actually a

convolution of the G-mode of sp^2-hybridized carbon and the D'-mode which represents short range order. Therefore, the Raman spectrum shows the first indication of the coexistence of diamond and a graphitic phase.

The following annealing temperature steps were set at 1100 °C and 1300 °C. In this range, the transformation noticeably continues, and the two characteristic bands of sp^2-hybridized carbon are clearly observed. The spectrum of the sample treated at 1100 °C has a D-band positioned at 1389.6 cm^{-1} and a G-band located at 1589.1 cm^{-1}, whereas the spectrum of the 1300 °C sample presents peaks at 1392.5 cm^{-1} and 1588.1 cm^{-1} of the D- and G band, respectively. In both cases, the extent of graphitization is significant. The full width at half maximum for the D- and G-bands are 124.5 cm^{-1} and 93.7 cm^{-1}, respectively. These values are in agreement with those reported by Zeiger et al. [11] and Cebik et al. [36], representing an increased long-range order of the sp^2 carbon.

An SEM/EDS analysis of the sample post-processed at 1300 °C is shown in **Figure 2**. The distribution of the particles is homogeneous on a 100 µm length scale. The carbon nanoparticle distribution ranges from aggregates of 100 nm up to several micrometers, which may be caused by the initial agglomeration of the nanodiamond powder.

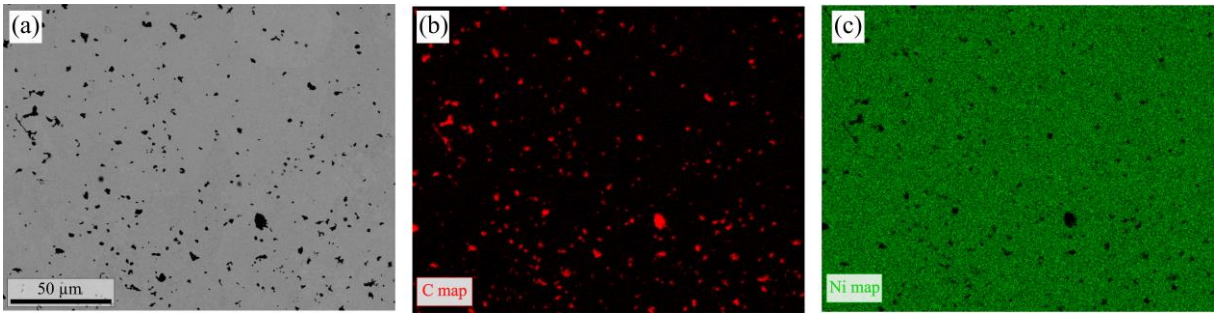

Figure 2 – (a) Secondary electron micrograph of the surface of the sample treated at 1300 °C. (b) EDS chemical map of the C distribution (in red) and (c) Ni distribution (in green).

Because of the synthesis method of the detonation nanodiamonds, dangling bonds may form at their surface. The latter can react and form covalent interparticle bonds, resulting in the development of agglomerates [37]. Such agglomerates cannot be dispersed by shear mixing or ultrasonication. Yet, these agglomerates are developed to a much lower degree than in case of carbon onions. If the latter are used as powder during mixing, the particles interaction due to the π-bonds are much more pronounced, leading to a strong re-agglomeration behavior after the dispersion process and during densification. The consequence would be the formation of larger agglomerates with an inhomogeneous distribution [8].

A morphological evaluation of the samples treated at 1300 °C is shown in **Figure 3**. It is clearly noticeable that there are still, at least, two different phases in the material (as observed in **Figure 3a**). Carbon onions are identified by their characteristic multi-shell architecture, whereas there are also small nanodiamond domains. The lattice distance obtained by a grayscale profile analysis (**Figure 3b**) coincides with the 0.34 nm spacing of graphitic structures ((002) plane). A third phase is identified as nickel with its characteristic lattice spacing matching the (111) plane (**Figure 3c**).

Some defective layers can be found on the outer shells, and disorder is noticeable in the inner space of the carbon onions. The former has been already reported in other works on the thermal annealing of nanodiamonds at 1300 °C and can be assigned to the presence of amorphous carbon [7,11]. The latter may be related to the stress increment in the interior of the carbon onion, derived from the volume change in the particle during the transformation. Carbon onions synthesized in this temperature range (750 – 1300 °C) show a defective inner structure resulting from the shortage of sp^3-hybridized atoms at the sp^3-sp^2 interface [38]. There is also a strong connectivity of the individual carbon particles. This neck formation has been reported, among others, by Zeiger et al. [11] and leads to aggregation of the particles.

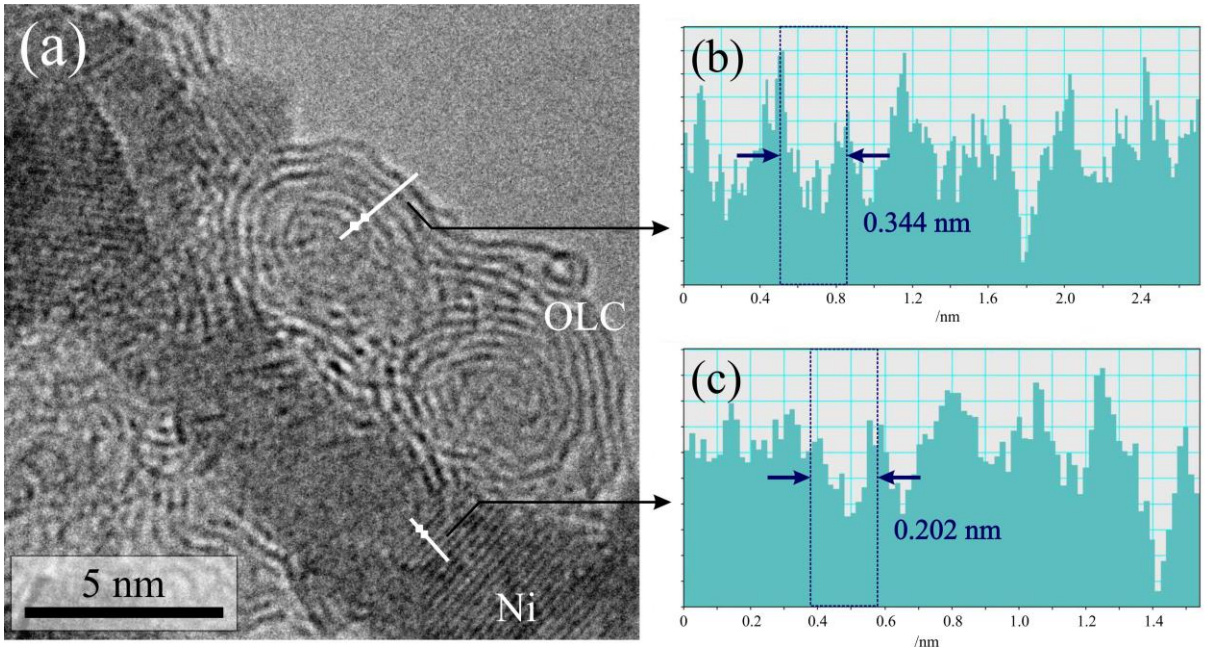

Figure 3 – (a) TEM image of the scratched material after thermal treatment at 1300 °C. (b) Grayscale line profile of a carbon onion, where the interplanar distance is in accordance to the (002) plane of graphitic carbon. (c) Grayscale line profile of a nickel domain, showing an interplanar distance corresponding to the (111) plane.

We used XPS to quantify the sp^2/sp^3 ratio for the samples which were treated at 750 °C and at 1300 °C (**Figure 4**). Based on the fitting procedure explained in the experimental section, the difference in binding energy of sp^2- and sp^3-bonded carbon is about 600 meV, which is comparable to the values reported in literature (e.g., 800 meV in Ref. [39]). For the 750 °C sample (**Figure 4a**), it is found that the particles contain sp^2 and sp^3 hybridized carbon atoms with a significant amount of C-O occurrence. This can be traced back to the detonation synthesis method of the nD [37]. Moreover, the appearance of incompletely crystallized carbon as outer shell of the nanodiamonds is well-known in literature, therefore explaining the relatively large relative amount of sp^2- hybridized carbon atoms [11]. The C=O bonding is also detected by Raman spectroscopy as side shoulder at 1760 cm^{-1}. In case of the sample which was post processed at 1300 °C (**Figure 4b**), a significant transformation can be observed.

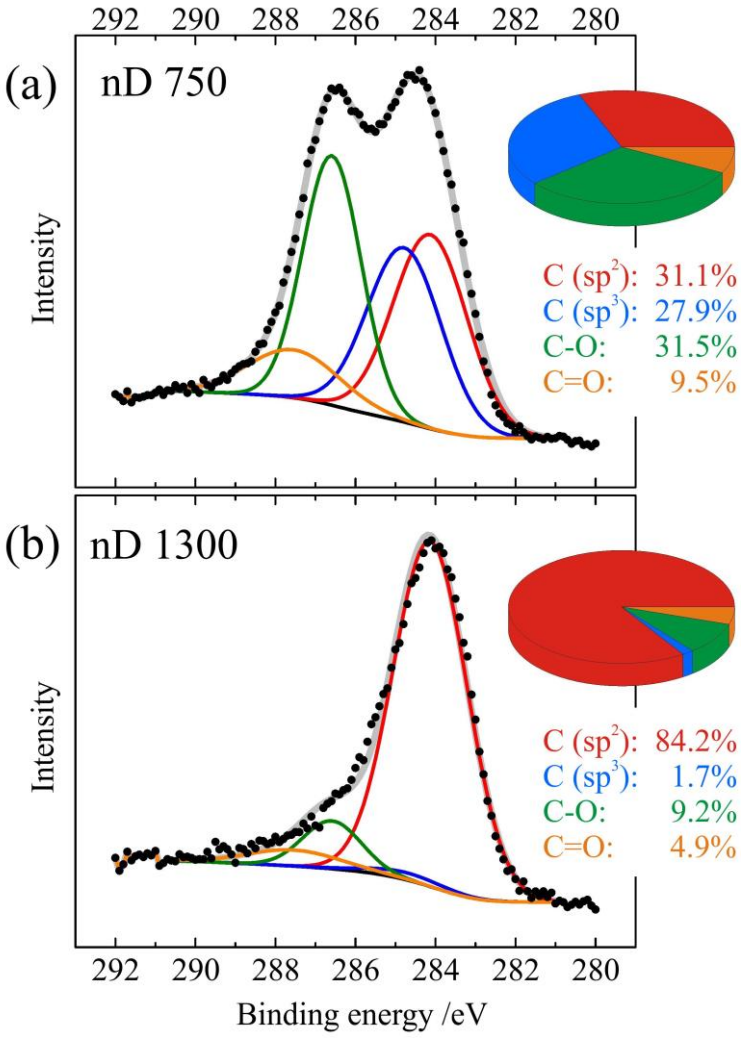

Figure 4 – (a) C-1s spectra of the sample treated at 750°C and, (b) at 1300°C with the corresponding distribution of carbon bonds on Shirley background.

With 84.2 at% of sp^2-hybridized carbon atoms, the particles seem to be largely graphitized, in agreement with the results from Raman spectroscopy and TEM analysis. A small fraction (1.7%) of sp^3 hybridized carbon is still detected. It must thus be mentioned that, by processing the composites with the conditions proposed in this study, it is possible to reduce significantly the nD fraction. However, there is still disordered domains within the carbon onions, which might need additional energy for their conversion, because of the stress generated by the volume expansion of the nanoparticle. Longer treatment times eventually result in larger transformation. However, transformation kinetics (conversion rates) in the analysed temperature range are low and strongly dependent on the original nD particle size (smaller nD convert faster) [38]. Yet, once the outer layers are converted, they become more difficult to rearrange and relieve generated stresses, thus possibly stabilizing a structurally disordered core region [38]. This would hinder the proper conversion, irrespective of the treatment time. In addition, we see a significant de-functionalization of the carbon nanoparticles, as the number of functional groups like C-O and C=O clearly decreases.

4. Conclusions

The transformation process of nanodiamond to carbon onions in a pre-densified nanodiamond-reinforced nickel matrix composite is studied. This is done by pressure-less, thermal annealing of the sintered sample under vacuum with temperatures ranging from 750 °C to 1300 °C. Raman spectroscopy measurements reveal that the sp^3 to sp^2 carbon ratio can be tuned by the annealing temperature. These results are confirmed by TEM analysis, showing the presence of carbon onions (with a disordered nucleus) dispersed in the nickel matrix after the annealing step at 1300 °C. The XPS data of the samples with the lowest and highest selected treatment temperatures demonstrates that the sp^2 carbon content of the particles increased from 31.1% (750 °C) up to 84.2% (1300 °C). Hence, it is demonstrated that it is possible to modify the sp^2 to sp^3 ratio within the metal matrix composite, simply by selecting the appropriate treatment temperature.

Acknowledgements

L. Reinert, S. Suarez, and F. Mücklich wish to acknowledge the EFRE Funds of the European Commission for support of activities within the AME- Lab project and the funding from the Deutsche Forschungsgemeinschaft (DFG, project: MU 959/38-1 and project: SU 911/1-1). This work was supported by the CREATe-Network Project, Horizon 2020 of the European Commission (RISE Project No. 644013). F. Müller and S. Grandthyll acknowledge funding

from the German Research Foundation (DFG) via the Collaborative Research Center SFB 1027. V. Presser and M. Zeiger kindly thank Prof. Eduard Arzt for his continuing support.

References

[1] Y. Gogotsi, V. Presser, Carbon Nanomaterials, 2nd ed., CRC Press, Boca Raton, FL, USA, 2013.

[2] V.N. Mochalin, O. Shenderova, D. Ho, Y. Gogotsi, The properties and applications of nanodiamonds, Nat. Nanotechnol. 7 (2012) 11–23. doi:10.1038/nnano.2011.209.

[3] V.L. Kuznetsov, Y. V. Butenko, A.L. Chuvilin, A.I. Romanenko, A. V. Okotrub, Electrical resistivity of graphitized ultra-disperse diamond and onion-like carbon, Chem. Phys. Lett. 336 (2001) 397–404. doi:10.1016/S0009-2614(01)00135-X.

[4] L. Wang, Y. Gao, Q. Xue, H. Liu, T. Xu, Effects of nano-diamond particles on the structure and tribological property of Ni-matrix nanocomposite coatings, Mater. Sci. Eng. A. 390 (2005) 313–318. doi:10.1016/j.msea.2004.08.033.

[5] V.Y. Dolmatov, T. Fudzhimura, G.K. Burkat, E.A. Orlova, Preparation of wear-resistant chromium coatings using nanodiamonds of different nature, Powder Metall. Met. Ceram. 42 (2003) 587–591. doi:10.1023/B:PMMC.0000022197.90234.f4.

[6] Y. Li, W.J. Zou, B.X. Li, Q.M. Dong, The Frictional Properties and Mechanism of Nano-Diamond/Ni Composite Coatings by Brush-Plating, Adv. Mater. Res. 291–294 (2011) 197–200. doi:10.4028/www.scientific.net/AMR.291-294.197.

[7] M. Zeiger, N. Jäckel, V.N. Mochalin, V. Presser, Review: carbon onions for electrochemical energy storage, J. Mater. Chem. A. 4 (2016) 3172–3196. doi:10.1039/C5TA08295A.

[8] L. Reinert, M. Zeiger, S. Suárez, V. Presser, F. Mücklich, Dispersion analysis of carbon nanotubes, carbon onions, and nanodiamonds for their application as reinforcement phase in nickel metal matrix composites, RSC Adv. 5 (2015) 95149–95159. doi:10.1039/C5RA14310A.

[9] A. Hirata, M. Igarashi, T. Kaito, Study on solid lubricant properties of carbon onions produced by heat treatment of diamond clusters or particles, Tribol. Int. 37 (2004) 899–905. doi:10.1016/j.triboint.2004.07.006.

[10] C. Portet, G. Yushin, Y. Gogotsi, Electrochemical performance of carbon onions, nanodiamonds, carbon black and multiwalled nanotubes in electrical double layer capacitors, Carbon N. Y. 45 (2007) 2511–2518. doi:10.1016/j.carbon.2007.08.024.

[11] M. Zeiger, N. Jäckel, M. Aslan, D. Weingarth, V. Presser, Understanding structure and

porosity of nanodiamond-derived carbon onions, Carbon N. Y. 84 (2015) 584–598. doi:10.1016/j.carbon.2014.12.050.

[12] Q. Zou, Y.G. Li, B. Lv, M.Z. Wang, L.H. Zou, Y.C. Zhao, Transformation of onion-like carbon from nanodiamond by annealing, Inorg. Mater. 46 (2010) 127–131. doi:10.1134/S002016851002007X.

[13] E. Falcao, F. Wudl, Review Carbon allotropes: beyond graphite and diamond, J. Chem. Technol. Biotechnol. 82 (2007) 524–531. doi:10.1002/jctb.

[14] P.K. Rohatgi, S. Ray, Y. Liu, Tribological properties of metal matrix-graphite particle composites, Int. Mater. Rev. 37 (1992) 129–152. doi:10.1179/imr.1992.37.1.129.

[15] L. Ru-Tie, X. Xiang, C. Fu-Sheng, L. Jin-Zhong, H. Li-Ling, Z. Yi-Qing, Tribological performance of graphite containing tin lead bronzesteel bimetal under reciprocal sliding test, Tribol. Int. 44 (2011) 101–105. doi:10.1016/j.triboint.2010.09.012.

[16] P. Rossi, S. Suarez, F. Soldera, F. Mücklich, Quantitative Assessment of the Reinforcement Distribution Homogeneity in CNT/Metal Composites, Adv. Eng. Mater. 17 (2015) 1017–1021. doi:10.1002/adem.201400352.

[17] S. Suarez, F. Lasserre, F. Soldera, R. Pippan, F. Mücklich, Microstructural thermal stability of CNT-reinforced composites processed by severe plastic deformation, Mater. Sci. Eng. A. 626 (2015) 122–127. doi:10.1016/j.msea.2014.12.065.

[18] L. Reinert, S. Suarez, T. Müller, F. Mücklich, Carbon Nanoparticle-Reinforced Metal Matrix Composites: Microstructural Tailoring and Predictive Modeling, Adv. Eng. Mater. 19 (2017) 1600750. doi:10.1002/adem.201600750.

[19] Q. Cheng, S. Debnath, E. Gregan, H.J. Byrne, Ultrasound-Assisted swnts dispersion: Effects of sonication parameters and solvent properties, J. Phys. Chem. C. 114 (2010) 8821–8827. doi:10.1021/jp101431h.

[20] F. Avilés, J. V. Cauich-Rodríguez, L. Moo-Tah, A. May-Pat, R. Vargas-Coronado, Evaluation of mild acid oxidation treatments for MWCNT functionalization, Carbon N. Y. 47 (2009) 2970–2975. doi:10.1016/j.carbon.2009.06.044.

[21] C. a Dyke, J.M. Tour, Solvent-free functionalization of carbon nanotubes., J. Am. Chem. Soc. 125 (2003) 1156–7. doi:10.1021/ja0289806.

[22] Y.-L. Zhao, J. Fraser Stoddart, Noncovalent Functionalization of Single-Walled Carbon Nanotubes, Acc. Chem. Res. 42 (2009) 1161–1171. doi:10.1021/ar900056z.

[23] L. Vaisman, H.D. Wagner, G. Marom, The role of surfactants in dispersion of carbon nanotubes, Adv. Colloid Interface Sci. 128–130 (2006) 37–46. doi:10.1016/j.cis.2006.11.007.

[24] H. Wang, Dispersing carbon nanotubes using surfactants, Curr. Opin. Colloid Interface Sci. 14 (2009) 364–371. doi:10.1016/j.cocis.2009.06.004.

[25] B. Munkhbayar, M.J. Nine, J. Jeoun, M. Bat-Erdene, H. Chung, H. Jeong, Influence of dry and wet ball milling on dispersion characteristics of the multi-walled carbon nanotubes in aqueous solution with and without surfactant, Powder Technol. 234 (2013) 132–140. doi:10.1016/j.powtec.2012.09.045.

[26] J.S. Gibson, J. Uddin, T.R. Cundari, N.K. Bodiford, A.K. Wilson, First-principle study of structure and stability of nickel carbides., J. Physics. Condens. Matter. 22 (2010) 445503. doi:10.1088/0953-8984/22/44/445503.

[27] M. Zeiger, N. Jäckel, D. Weingarth, V. Presser, Vacuum or flowing argon: What is the best synthesis atmosphere for nanodiamond-derived carbon onions for supercapacitor electrodes?, Carbon N. Y. 94 (2015) 507–517. doi:10.1016/j.carbon.2015.07.028.

[28] A. Ferrari, J. Robertson, Interpretation of Raman spectra of disordered and amorphous carbon, Phys. Rev. B. 61 (2000) 14095–14107. doi:10.1103/PhysRevB.61.14095.

[29] S. Osswald, V.N. Mochalin, M. Havel, G. Yushin, Y. Gogotsi, Phonon confinement effects in the Raman spectrum of nanodiamond, Phys. Rev. B - Condens. Matter Mater. Phys. 80 (2009). doi:10.1103/PhysRevB.80.075419.

[30] G.N. Yushin, S. Osswald, V.I. Padalko, G.P. Bogatyreva, Y. Gogotsi, Effect of sintering on structure of nanodiamond, Diam. Relat. Mater. 14 (2005) 1721–1729. doi:10.1016/j.diamond.2005.06.030.

[31] S. Osswald, G. Yushin, V. Mochalin, S.O. Kucheyev, Y. Gogotsi, Control of sp2/sp3 Carbon Ratio and Surface Chemistry of Nanodiamond Powders by Selective Oxidation in Air, J. Am. Chem. Soc. 128 (2006) 11635–11642. doi:10.1021/ja063303n.

[32] V.L. Kuznetsov, Y. V Butenko, Diamond phase transitions at nanoscale, in: Ultrananocrystalline Diam., 2nd Ed., Elsevier Inc., 2012: pp. 181–244. doi:10.1016/B978-1-4377-3465-2.00007-4.

[33] J.K. McDonough, A.I. Frolov, V. Presser, J. Niu, C.H. Miller, T. Ubieto, M. V. Fedorov, Y. Gogotsi, Influence of the structure of carbon onions on their electrochemical performance in supercapacitor electrodes, Carbon N. Y. 50 (2012) 3298–3309. doi:10.1016/j.carbon.2011.12.022.

[34] S. Suarez, F. Lasserre, F. Mücklich, Mechanical properties of MWNT/Ni bulk composites: Influence of the microstructural refinement on the hardness, Mater. Sci. Eng. A. 587 (2013) 381–386. doi:10.1016/j.msea.2013.08.058.

[35] N.S. Xu, J. Chen, S.Z. Deng, Effect of heat treatment on the properties of nano-

diamond under oxygen and argon ambient, Diam. Relat. Mater. 11 (2002) 249–256.

[36] J. Cebik, J.K. McDonough, F. Peerally, R. Medrano, I. Neitzel, Y. Gogotsi, S. Osswald, Raman spectroscopy study of the nanodiamond-to-carbon onion transformation., Nanotechnology. 24 (2013) 205703. doi:10.1088/0957-4484/24/20/205703.

[37] A. Pentecost, S. Gour, V. Mochalin, I. Knoke, Y. Gogotsi, Deaggregation of nanodiamond powders using salt- and sugar-assisted milling, ACS Appl. Mater. Interfaces. 2 (2010) 3289–3294. doi:10.1021/am100720n.

[38] O.A. Shenderova, D.M. Gruen, eds., Ultrananocrystalline Diamond: Synthesis, Properties, and Applications, 1st ed., William Andrew Publisher, Norwich, NY, USA, 2006.

[39] P. Mérel, M. Tabbal, M. Chaker, S. Moisa, J. Margot, Direct evaluation of the sp3 content in diamond-like-carbon films by XPS, Appl. Surf. Sci. 136 (1998) 105–110. doi:10.1016/S0169-4332(98)00319-5.